

INFLUENCE OF LOCAL AND LATERAL BUCKLING  
ON INELASTIC BEHAVIOR OF STEEL FRAMES

By Chiaki MATSUI (I), Takashi YOSHIKUMI (II)

SUMMARY In order to clarify the influence of the local and lateral buckling on the inelastic behavior of mild steel frames, the portal frame specimens are tested under the constant vertical and monotonic or alternating horizontal loads. Deformation capacity and energy absorption capacity are investigated, and it is shown that experimental behavior of the locally buckling frames is well predicted by the analysis.

INTRODUCTION

In seismic design, it is very important to ascertain by the dynamic analysis that the designed structure shows a sufficient performance under strong earthquake motion, and thus the restoring force characteristics used in the dynamic analysis are needed to be realistic. The authors have investigated the influence of the instability due to  $P-\Delta$  moment and of the material properties on the restoring force characteristics of steel frames in which the local or lateral buckling does not take place, and reported the results at the past WCEE [1,2,3]. Recently, a few researches [4,5,6] have been reported on the influence of local and lateral buckling on the carrying capacity and the post-buckling behavior of a single member. However, no research can be found on the inelastic behavior of a frame containing locally and/or laterally buckling members.

In this study, mild steel portal frame specimens are tested under the constant vertical and monotonic or alternating horizontal loads. Experimental behavior of the frames is compared with the analytical results based on the plastic hinge method in which the decrease of the full plastic moment of the cross section due to the local buckling is taken into consideration.

TEST PROGRAM

The test program consists of two series of portal frame specimens (mild steel SS41, Japanese Industrial Standards); the one investigating the influence of the local buckling (L-series), and the other the lateral buckling (T-series). The frame specimens assembled by welding from built-up H-shape columns (Fig.1) and a rolled H-shape beam (H-100x100x6x8) are tested under the monotonic or alternating horizontal load  $H$ , in addition to the constant vertical loads on the columns  $P'$  and the center of the beam  $W$  (Fig.2). The load  $W$  on the beam is determined so that maximum stress occurring in the frame under the vertical loads only is equal to two-thirds of the yield strength of the material. The frame collapses in the sway mechanism. Figure 3 shows the loading arrangement. As the experimental parameters,  $b/t_f$ ,  $d/t_w$ ,  $h \cdot d/A_f$  and  $n=P/P_y$  are selected. The values of these parameters are shown in Table 1 together with notation for symbols. The specimen name is indicated in the form of  $\boxed{A} \boxed{B} - \boxed{C} \boxed{D}$ , where A stands for series name, B loading condition (M=monotonic, R=repeated loading), C column cross section,

---

(I) Associate Professor, Faculty of Engineering, Kyushu University, Fukuoka, Japan

(II) Research Assistant, Faculty of Engineering, Kyushu University

and D axial load ratio ( $n=0.1, 0.3$  and  $0.6$ , when  $D=1, 2$  and  $3$ , respectively). Totally thirty eight specimens are tested; the local buckling of columns takes place in twenty six of them, and the lateral buckling in twelve.

#### TEST RESULTS

Examples of the experimental behavior of the frames are shown in Figs. 4 and 6. Definition of symbols used is given in Fig.5, where the mechanism line is obtained on the assumption that the sway mechanism forms when the column moments at the base and at the face of the beam-to-column connection reach  $M_{pc}$ , the full plastic moment reduced by the axial force. Figure 7 shows the relations between the deformation capacity  $R$  defined in Fig.8 and  $(b/t_f) \cdot \sqrt{\sigma_y}$ , and the relations between the accumulated energy  $\sum W_i / (H_{PN} \cdot \Delta_{PN})$  and plastic displacement  $\sum \Delta_i / \Delta_{PN}$  are shown in Fig.9, where definition of symbols is given in Fig.10. When evaluating  $W_i$  and  $\Delta_i$  in each cycle of loading, these hysteretic loops are taken where the carrying capacity exceeds 90% of the maximum load carrying capacity that the specimen has experienced. The following observations are made from the test results of L-series: (1) Deterioration of the restoring force is remarkable as the values of  $b/t_f$ , and  $d/t_w$  become large. A considerable deterioration starts at the occurrence of web local buckling induced after flange local buckling. This phenomenon is more pronounced with the increase in the value of  $n$ . (2) Deformation capacity defined by the value of the displacement at the maximum horizontal load does not so much depend on the ratio  $d/t_w$  as on  $b/t_f$  (Fig.7). (3) Energy absorption capacity becomes smaller as the ratios  $b/t_f$  and  $d/t_w$  become large (Fig.9.1). Furthermore, the following observations are made from the test results of T-series: (4) With the increase in the values of  $h \cdot d / A_f$  and  $n$ , the out-of-plane deformation becomes large and deterioration of the restoring force is remarkable (Figs.4.4-4.6), and then energy absorption capacity becomes smaller (Fig.9.2).

#### THEORETICAL PREDICTION

Test frames are analysed by the plastic hinge method, considering the shear deformation. In the analysis, a piecewise linear relation is assumed between the resisting moment  $M$  and the rotation  $\theta$  at the plastic hinge, as shown by dashed lines in Fig.11, which approximates the experimental results of locally buckling beam-columns [7]. From this approximation, the relation between the increments of the resisting moment  $\Delta M$  and the rotation  $\Delta \theta^P$  of the plastic hinge is expressed as follows;  $\Delta M = \tau \cdot \Delta \theta^P$  in which  $\tau = a$  constant, obtained from a piecewise linear approximation in Fig.11. Results of the frame analysis are shown in Fig.12, and the present analysis can predict well the overall behavior of the locally buckling frames.

#### DISCUSSION AND CONCLUSION

The restoring force characteristics of portal frames are investigated experimentally under the monotonic and alternating horizontal loads. Test results show that the deterioration of the restoring force is remarkable as the values of  $b/t_f$ ,  $d/t_w$  and  $h \cdot d / A_f$  become large, and this phenomenon is more pronounced with the increase in the value of  $P/P_y$ . Thus the deformation capacity of steel frames under earthquake motion varies with the values of the parameters mentioned above, and a definite value of the deformation capacity cannot be determined unconditionally. Consequently, the relation

shown in Fig.7 may be helpful to know allowable deformation of real frame. The present analysis can predict well the characteristics of the locally buckling frames, in spite of its simplicity. Further study is needed to predict the behavior of laterally buckling frames.

#### ACKNOWLEDGMENT

The authors wish to express their gratitude to Dr. S. Morino, Assoc. Prof., Kyushu Univ. for valuable discussion and assistance.

#### REFERENCES

- [1] M. Wakabayashi, T. Nonaka and C. Matsui: AN EXPERIMENTAL STUDY ON THE HORIZONTAL RESTORING FORCES IN FRAMES UNDER LARGE VERTICAL LOADS, Proc. 4th WCEE, Santiago, Vol. I, B-2, Jan., 1969, pp. 177-193.
- [2] M. Wakabayashi, C. Matsui, K. Minami and I. Mitan: INELASTIC BEHAVIOR OF STEEL FRAMES SUBJECTED TO CONSTANT VERTICAL AND ALTERNATING HORIZONTAL LOADS, Proc. 5th WCEE, Rome, Vol. I, June 1974, pp. 1194-1197.
- [3] C. Matsui and I. Mitan: INELASTIC BEHAVIOR OF HIGH STRENGTH STEEL FRAMES SUBJECTED TO CONSTANT VERTICAL AND ALTERNATING HORIZONTAL LOADS, Proc. 6th WCEE, Vol. III, New Delhi, 1977, pp. 3169-3174.
- [4] J.J. Climehage and R.P. Johnson: MOMENT ROTATION CURVES FOR LOCALLY BUCKLING BEAMS, Proc. ASCE, Vol. 98, No. 576, June 1972, pp. 1239-1254.
- [5] W.P. Vann, L.E. Thompson, L.E. Whally and L.D. Ozier: CYCLIC BEHAVIOR OF ROLLED STEEL MEMBERS, Proc. 5th WCEE, Vol. I, Rome, 1974, pp. 1187-1193.
- [6] I. Mitan, M. Makino and C. Matsui: INFLUENCE OF LOCAL BUCKLING ON CYCLIC BEHAVIOR OF STEEL BEAM-COLUMNS, Proc. 6th WCEE, Vol. III, New Delhi, 1977, pp. 3175-3180.
- [7] M. Makino, C. Matsui and I. Mitan: POST LOCAL BUCKLING BEHAVIOR OF STEEL BEAM-COLUMNS PART I TEST PROGRAM AND TEST RESULTS, Trans. Architect. Inst. of Japan, No. 281, July, pp. 71-80 (in Japanese).

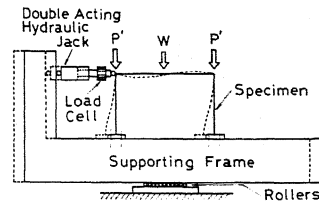
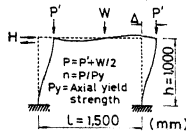
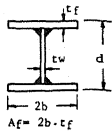


Fig.1 Column Section Fig.2 Loading Condition

Table 1 Experimental Parameters

Specimen Name	Column Member (mm)	$h/t_f$	$d/t_w$	$hd/A_f$	$h/i_x$	$h/i_y$
L-1	H-100x100x6x8	6.3	16.7	125	23.9	40.5
L-2	BH-100x100x3.2x6	8.3	31.3	167	22.9	38.8
L-3	BH-135x100x3.2x6	8.3	42.2	225	17.0	40.2
L-4	BH-100x100x3.2x4.5	11.1	31.3	222	23.0	40.2
L-5	BH-100x100x3.2x3.2	15.6	31.3	313	23.4	42.4
L-6	BH-135x100x3.2x3.2	15.6	42.2	422	17.7	44.8
T-1	BH-100x50x3.2x6	4.2	31.3	333	24.2	84.7
T-2	BH-100x50x3.2x3.2	7.8	31.3	625	25.1	98.0

2b,  $t_f$ , d,  $t_w$  = width and thickness of flange, depth of the cross section, and thickness of web, respectively;  $A_f$  = cross sectional area of the flange; h = story height;  $i_x$ ,  $i_y$  = radii of gyration about strong and weak axes, respectively.

Fig.3 Loading Arrangement

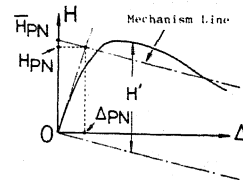


Fig.5 Definition of Symbols

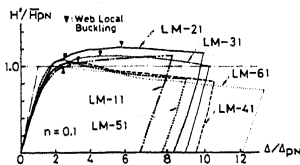


Fig.4.1

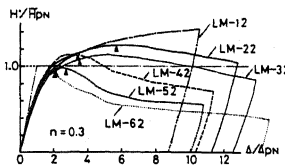


Fig.4.2

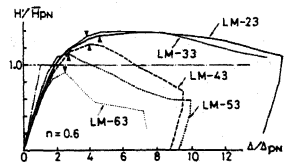


Fig.4.3

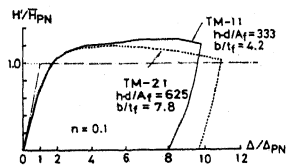


Fig.4.4

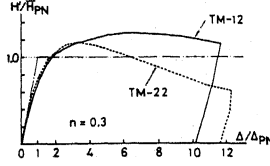


Fig.4.5

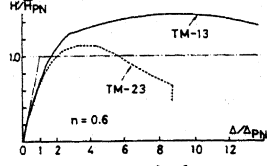


Fig.4.6

Fig.4 Experimental Results under Monotonic Horizontal Load

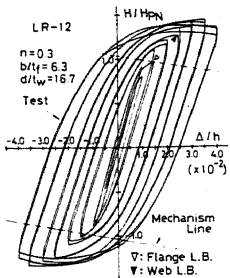


Fig. 6.1

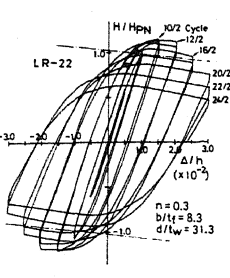


Fig. 6.2

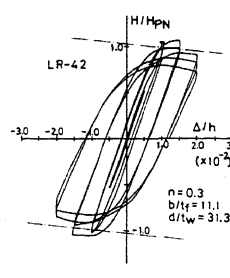


Fig. 6.3

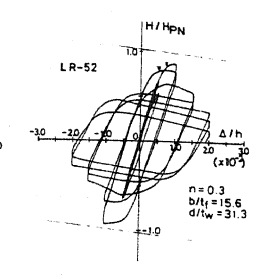


Fig. 6.4

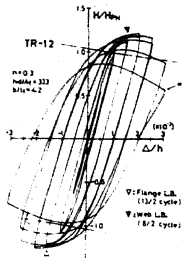


Fig. 6.5

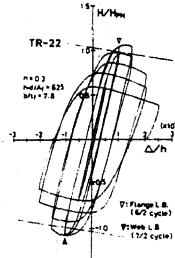


Fig. 6.6

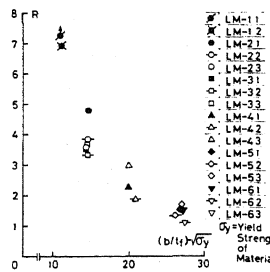


Fig. 7 Deformation Capacity

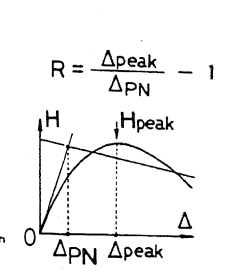


Fig. 8 Definition of R

Fig. 6 Experimental Results under Alternating Horizontal Load

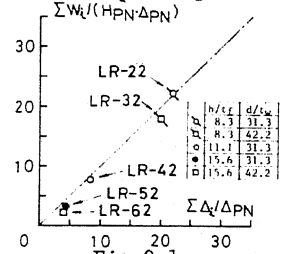


Fig. 9.1

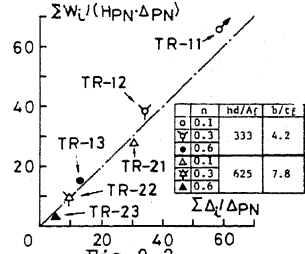


Fig. 9.2

Fig. 9 Accumulated Energy and Plastic Displacement

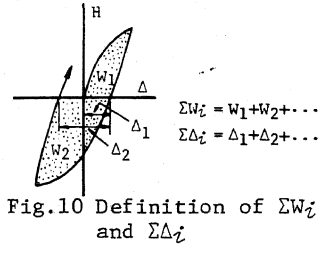


Fig. 10 Definition of ΣW<sub>i</sub> and ΣΔ<sub>i</sub>

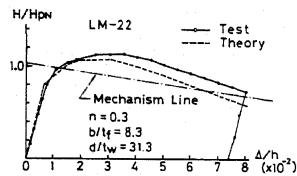


Fig. 12.1

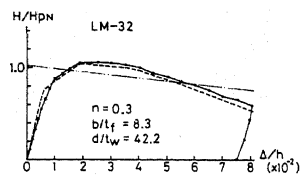


Fig. 12.2

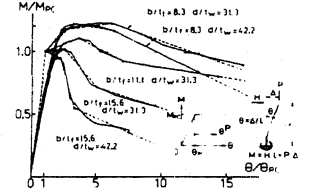


Fig. 11 Experimental M-θ Relations

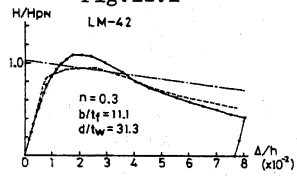


Fig. 12.3

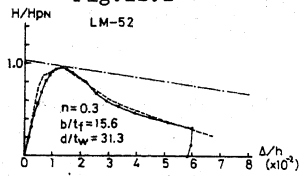


Fig. 12.4

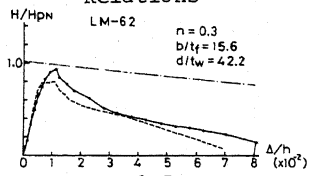


Fig. 12.5

Fig. 12 Comparison of Test and Analytical Results